B-VHF – SELECTED SIMULATION RESULTS AND ASSESSMENT

S. Brandes, M. Schnell, German Aerospace Center, DLR Oberpfaffenhofen, 82234 Wessling, Germany
C.-H. Rokitansky[1], M. Ehammer, Th. Gräupl, University of Salzburg, 5020 Salzburg, Austria
H. Steendam, M. Guenach, TELIN Department, Ghent University, Ghent, Belgium
C. Rihacek, B. Haindl, Frequentis GmbH, Wolfganggasse 58-60, 1120 Vienna, Austria

Abstract

B-VHF is a proposal for a future aeronautical communication system in the VHF band based on an overlay concept, i.e. during the transition phase the B-VHF system shares the same frequency band with legacy VHF systems without interfering with them. In this paper, the overlay concept is evaluated by simulations of the physical and higher layers. Simulation results show that the B-VHF overlay system works in presence of interference from legacy VHF systems. The protocol is designed to allow using the available resources very efficiently and to provide voice and data services with the required quality of service.

I Introduction

B-VHF ("Broadband VHF Aeronautical Communications System Based on Multi-carrier Technology") [1] is a research project co-funded by the European Commission which has started in January 2004 and is finalized in September 2006. The main goal of the B-VHF project is to verify the feasibility of a multi-carrier based overlay system for future air traffic control (ATC) communications in the very high frequency (VHF) band operating simultaneously with legacy VHF systems without causing interference. This approach enables in-band transition from the current to a future ATC communications system and, thus, allows future ATC communications to stay in the advantageous and protected VHF band.

The B-VHF overlay concept has already been presented at DASC 2004 [2], and in 2005, the physical (PHY) layer design of B-VHF has been detailed [3] with special emphasis on co-existence issues between B-VHF and the legacy VHF systems. At this year's conference, right after the end of the current project, the results of the B-VHF system simulations are presented and an assessment about the feasibility of the overlay concept in the VHF band is given.

In a first step, the performance of the PHY layer is assessed using a set of realistic simulation scenarios. These scenarios comprise different channel conditions according to the different phases of flight, e.g., take-off and landing, taxiing, parking, or en-route flights. Moreover, realistic as well as worst-case situations for the interference from the legacy VHF systems towards the B-VHF system are taken into account.

In a second step, higher layer protocol simulations are performed using the results from the physical layer simulations to model the B-VHF air interface, the interference situation in the VHF band, and the propagation conditions of the channel. Voice and different data applications are considered and the overall B-VHF system performance is assessed with respect to relevant system parameters like delay and throughput.

The remainder of this paper is organized as follows. In Section II, PHY layer simulations are addressed. This section contains a description of the system model including the most important components specific for an overlay system as well as the considered simulation scenarios. Section III deals with the assessment of the developed data link layer (DLL) and higher layers protocols. In this section, the simulated system model and the simulation setup used for evaluating the protocols are described. In Section IV, simulation results for the PHY layer as well as for the DLL protocols are presented. In the last section, the B-VHF overlay concept is assessed and conclusions are drawn.

[1] Main affiliation: RWTH Aachen University / Communication Networks

1-4244-0378-2/06/$20.00 ©2006 IEEE.

II PHY Layer Assessment

The B-VHF system is designed as an overlay system, i.e. the B-VHF system shares the same frequency band with legacy VHF systems without interfering with them. In Figure 1, the spectrum allocation of the VHF band is shown schematically. Some 25 kHz or 8.33 kHz channels are occupied by the analog voice communication system using double sideband amplitude modulation (DSB-AM) or by digital data communication systems like VHF digital link (VDL) Mode 2. Idle VHF channels are used by the B-VHF system that adapts its transmission signal to the current spectrum allocation. With OFDM this is easily realized by turning on or off the corresponding subcarriers.

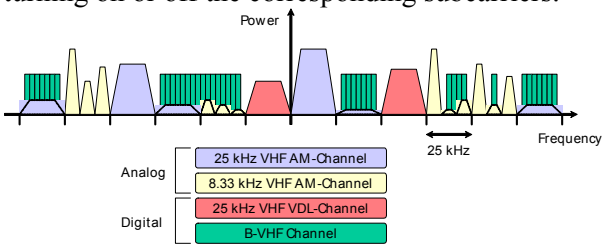

Figure 1. B-VHF overlay concept – using frequency gaps in the VHF band.

System Model

A bandwidth of 1 MHz corresponding to 40 VHF channels is assigned to each B-VHF cell. The subcarrier spacing is chosen such that 12 OFDM subcarriers lie in one VHF channel with 25 kHz bandwidth, i.e. Δf=2.083 kHz. In the forward link (FL), i.e. ground station (GS) to aircraft (A/C), OFDM is combined with spreading resulting in a multi-carrier code-division multiple-access (MC-CDMA) system. In the reverse link (RL), i.e. A/C to GS, orthogonal frequency-division multiple-access (OFDMA) is applied.

The simplified block diagram for the FL in Figure 2 reveals that a conventional OFDM based system has to be extended by only a few blocks to obtain an OFDM based overlay system. The frame composer has to be modified such that the OFDM signal can be adapted to the currently available VHF channels. Moreover, a block for suppressing the OFDM sidelobes is inserted in order to minimize the influence on legacy VHF systems. This is e.g. realized by inserting cancellation carriers that carry weighting factors optimized to cancel the sidelobes of the original transmit signal [3]. Sidelobes can also be reduced by windowing the transmit signal in time domain.

The B-VHF signal is transmitted over a multi-path channel. In contrast to conventional OFDM systems it is not only affected by noise, but also by interference from legacy VHF systems. Two kinds of interferers have to be distinguished. VHF stations in the proximity of the B-VHF system cause *strong interference*. These systems do not operate in VHF channels that are used by the B-VHF overlay system; nevertheless they have a significant influence of the B-VHF system. In those channels that are used by the B-VHF system *weak interference* occurs. The corresponding VHF stations are not in the proximity of the B-VHF system; hence, these VHF stations are not affected by the B-VHF system. In return, these VHF stations cause interference on B-VHF subcarriers.

At the B-VHF receiver, the influence of narrow-band interference (NBI) from other VHF systems has to be mitigated. Apart from that, appropriate algorithms for time and frequency synchronization are chosen, that work properly despite NBI and gaps in the synchronization symbol. Methods for that are briefly described in the following.

Interference Mitigation

At the B-VHF receiver, NBI originating from legacy VHF systems has to be mitigated in order to minimize its impact on the performance of the B-VHF system. The different approaches for NBI mitigation can be applied at different positions in the B-VHF receiver: analog time domain, digital time domain, and/or digital frequency domain.

In order to avoid a saturation of the signal at the A/D converter, very strong interferers have to be reduced e.g. by notch filters. Notch filtering is a very effective technique for NBI mitigation. However, in an overlay system the dynamic adaptation of the filter characteristics to the changing spectrum allocation is very complex, as depending on the currently used B-VHF cell, the number and position of the required notches varies. Consequently, analog notch filters are only applied for very strong interferers, if it can not be avoided. Note, notch filters can also be applied in digital domain when the resolution of the A/D converter is high enough to avoid a saturation of the signal.

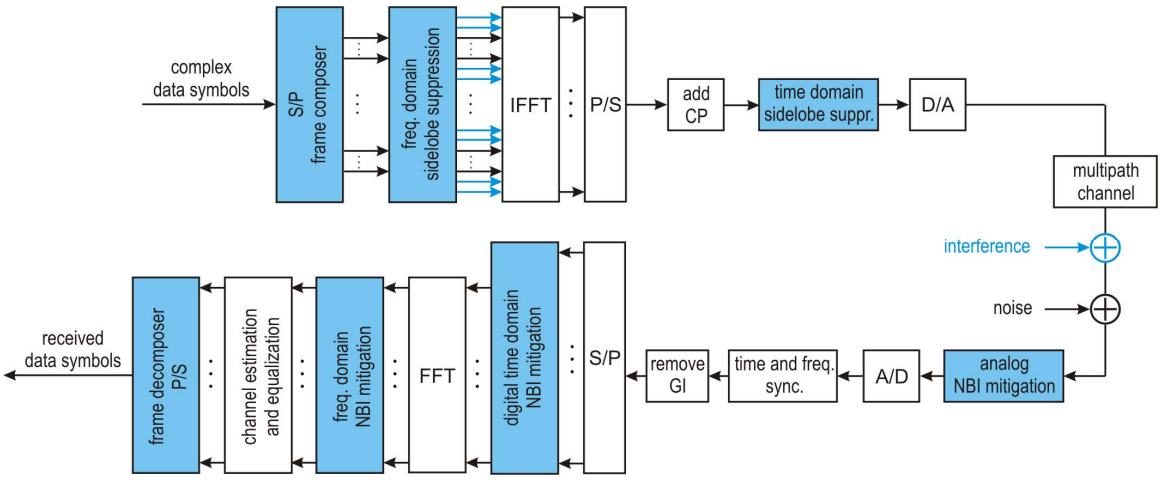

Figure 2. Simplified block diagram of FL system, blocks required for overlay system highlighted.

After A/D conversion the remaining interference is further reduced in digital time domain by windowing the Rx signal with a windowing function that differs from the normally implicitly applied rectangular window. Commonly used windows are Hamming, Hann, or raised-cosine shapes. If the width of the window has to be chosen such that only the interference part of the signal is influenced, whereas the data part remains unchanged [4]. The windowing operation can be implemented easily, as it is based on a simple multiplication of the Rx signal and no knowledge about interference is required. However, the OFDM signal has to be extended in time domain resulting in a slightly reduced system throughput.

After the FFT the leakage effect occurs, i.e. the interference signal, that is originally narrow and spans only 3-4 subcarriers, is spread over the complete transmission bandwidth. Hence, all OFDM subcarriers are affected by this NBI signal. As the leakage effect is a deterministic property of the FFT, the influence of the NBI signal can be reconstructed and minimized. Therefore, NBI is measured on a few observation subcarriers located close to the center frequency of the interferer. Based on the estimated and reconstructed NBI signal a compensation matrix is determined that minimizes the mean square error on each subcarrier [5]. In case of strong interferers all 12 subcarriers in the corresponding channel may serve as observation subcarriers. In case of weak interferers a few data subcarriers have to be sacrificed for observation purposes. However, only one observation subcarrier per 25 kHz channel is satisfying.

Synchronization

In typical multi-carrier systems, carrier frequency synchronization is required when the carrier frequency offset is larger than 5% of the carrier spacing [6]. In the B-VHF system with carrier spacing 2.083 kHz, the maximum expected Doppler frequency f_D for all scenarios is only a small fraction of the carrier spacing (see Table 1). Hence, carrier frequency synchronization is not a crucial issue in the B-VHF system, especially when the channel equalizer is able to track the slow channel changes caused by the Doppler. This conclusion is confirmed by simulation results.

Table 1. Maximum Doppler frequency for different flight scenarios.

	Parking	**Take-off/ Landing**	**En-route**
f_D (Hz)	2.3	65.0	120.0

For FL timing synchronization, two synchronizers are considered. The first synchronizer is the data aided (DA) maximum likelihood (ML) synchronizer [7]. The DA ML synchronizer makes use of the signal structure and requires the knowledge of certain system parameters like e.g. the positions of the carriers used by the B-VHF system. Note that this timing synchronizer is not suitable for the net entry phase, where this information on the signal is not available. Therefore, for the net entry phase, another timing synchronizer is used, i.e. the algorithm proposed by Schmidl and Cox (S&C) [8]. In this algorithm,

certain symmetry in the time domain of the pilot synchronization symbols is assumed. While the S&C synchronizer is only used in the net entry phase, the DA ML synchronizer can be used to update the timing estimates regularly when the timing estimates obtained with S&C are not good enough to obtain an acceptable performance. Both the DA ML and the S&C synchronizer can use the same pilot synchronization symbols that are added as a preamble to the FL frame. However, the DA ML synchronizer can easily be extended to also use the pilot symbols that are available in the data section of the FL frame to estimate the channel.

After the A/C has obtained the FL timing synchronization and the signal structure, it can start to transmit in the random access channel (RACH) to set up a communication link with the GS. The GS uses the signal sent by the A/C in the RACH to estimate the timing of the A/C with the DA ML synchronizer proposed for the FL. The GS then sends information about the timing back to the A/C in a FL frame, such that the A/C is able to adapt its RL timing.

Simulation Setup

For assessing the B-VHF overlay concept the performance of the PHY layer is evaluated in presence of NBI. For all simulations the FL is considered. In order to evaluate the B-VHF system in different flight phases two different en-route scenarios (a typical scenario (FL-ENR) and a worst case scenario (FL-WC)), a take-off/landing scenario (FL-TOFF) as well as a parking scenario (FL-Park) are considered. The NAVSIM tool [1], which simulates the available VHF channels under worst case assumptions, is used to select that 1 MHz band with the smallest number of interferers. The band from 136-137 MHz is chosen for three of the scenarios: FL-ENR, FL-TOFF, and FL-PARK. In this 1 MHz band 13 channels are available for the B-VHF system in one of the most congested area in Europe. The remaining channels are possibly used by legacy VHF systems and hence excluded for the B-VHF system. The actual interference is modeled according to the results retrieved from the measurement campaign. As the same procedure is applied for frequency planning of the B-VHF system, a realistic interference situation is obtained this way. In addition, a worst case en-route (FL-WC) interference situation is simulated. According to results from the measurement flights the range from 119.65 to 120.65 MHz is the 1 MHz band with the maximum number of interferers in the measured scenarios. The resulting spectrum allocation for the chosen 1 MHz bands for different scenarios is depicted in Table 2.

Table 2. Spectrum allocation for different simulation scenarios.

Scenario	Spectrum Allocation
FL-PARK	
FL-TOFF	
FL-ENR	
FL-WC	
strong interferer weak interferer	B-VHF channel idle channel

In Table 3, the average total interference power $P_{I,av}$ for each scenario is calculated from the average powers $P_{I,S}$ and $P_{I,W}$ of each weak and strong interferer considering the duty cycles η_S and η_W. Moreover, the number of available data subcarriers is given. This number is derived from the number of available VHF channels under the assumption that two cancellation carriers for sidelobe suppression are inserted at each edge of the B-VHF spectrum. For each scenario the channel is simulated with a model derived from the channel measurement campaign [1]. In all scenarios a guard interval of 10 samples equivalent to about 10 µs is sufficient to compensate multi-path propagation delays.

Table 3. Parameters for the different simulation scenarios.

	FL-PARK	FL-TOFF	FL-ENR	FL-WC
N_c	116	116	116	384
N_I	1S/1W	1S/2W	2S/2W	6S/7W
$P_{I,S}$ (dBm)	-55.20	-71.77	-78.36	-78.36
η_S (%)	18.43	18.72	25.28	25.28
$P_{I,W}$ (dBm)	-83.98	-88.52	-83.57	-83.57
η_W (%)	4.15	5.05	7.47	7.47
$P_{I,av}$ (dBm)	-62.54	-79.00	-80.95	-76.12

In order to allow for a fair comparison between the different scenarios, the same system parameters as specified in the B-VHF system design are used in all simulations. As already mentioned the system bandwidth is 1 MHz, corresponding to 480 subcarriers. The length of the FFT is 512. In the FL, MC-CDMA with spreading length L=4 is used, i.e. in the FL-PARK, FL-TOFF, and FL-ENR scenario, each user has 29 data symbols per OFDM symbol. In all simulations, a fully loaded system is assumed.

One OFDM frame consists of 42 symbols and one synchronization symbol at the beginning. As described above, for synchronization in the FL the ML algorithm is applied. For channel estimation pilot symbols are inserted after every forth OFDM symbol. As the pilot symbols have one pilot tone on each used subcarrier, only a linear interpolation in time domain is required. At the B-VHF receiver, the influence of NBI is mitigated by a Hann window with a roll-off factor according to μ=26 additional samples. Finally, minimum mean square error (MMSE) detection is performed.

For simulating different applications, modulation scheme and coding rate are adapted to the transmission of voice, data, and headers. For voice uncoded QPSK, for data QPSK with a convolutional code with coding rate R=1/2, and for the headers QPSK with Golay coding with R=1/2 is transmitted.

III DL Layer Assessment

B-VHF supports two different types of communication. The protocol has been designed to provide native support for digital voice communication and a general purpose digital data link. While each of these transmission modes can be used on its own, the protocol supports the simultaneous operation of both of them.

This feature is accomplished by combining the multi-carrier characteristic of the B-VHF system with a time-division multiple-access (TDMA) scheme. This timing mechanism is under the control of a local GS managing all B-VHF communication within a designated area, i.e. a B-VHF cell. Within this cell direct communication occurs only between A/C and GS. A/C to A/C communication is established indirectly by the GS via a relay mechanism.

Timing Structure

The B-VHF timing structure is organized as a sequence of *super frames*. Each super frame (Figure 3) has a length of 240 ms and starts with a *broadcast slot* (BC) followed by two odd and two even *multi frames* (MF). The BC slot is used by the GS for the public announcement of management data relating to its cell. The MFs consist of three (or four) slots of different type. Each slot type is associated with a link direction. The FL slot is used for ground to air communication, the RL slot for air to ground transmission.

Each MF contains a FL slot and a RL slot. These slots are reserved for user data and extra management information not published on the BC. Both of these slots are under the authority of the GS and an A/C wishing to send data frames has to make a reservation at the GS first.

The odd MF contains a *random access* (RA) slot, used for the synchronization of newly arriving A/C at the cell. The even MF contains two *synchronized random access* (sRA) slots, which are used for resource acquisition. If the A/C succeeds in getting synchronized the GS grants the desired resources by issuing a resource reservation on one of the FL slots.

For each of the time slots different kinds of physical channels are used. If the available spectrum allows the usage of multiple physical channels appropriate channels may be combined to increase the capacity of the respective time slot, i.e. each slot combines as many physical carriers as possible. Table 4 gives an overview of the mapping between physical transport channels and transport channels and their slot in the timing structure.

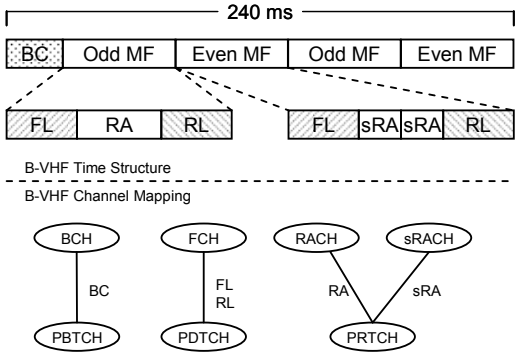

Figure 3. B-VHF super frame.

Table 4. B-VHF transport channels.

Transport Channel	Mapping on time structure	Physical Transport Channel	Direction
BCH	BC	PBTCH	GS→A/C
RACH	RA	PRTCH	A/C→GS
sRACH	sRA		
FCH	FL or RL	PDTCH	A/C↔GS

Synchronization

An A/C operating in a B-VHF cell can be in one of three different synchronization states. The synchronization state constraints the communication ability of an A/C. Which state it is in depends on how accurate the time advance and frequency adaptation of an A/C is.

It is assumed that all neighboring B-VHF GSs are synchronized in time. Further on it is anticipated that an external time source is providing an absolute time to a B-VHF GS in regular time intervals.

The different synchronization states are:

- A/C SS 0 – Unsynchronized.
- A/C SS 1 – Synchronized on FL.
- A/C SS 2 – Synchronized on FL & RL.

Achieving A/C SS 1 is accomplished through procedures described in Section II. This state enables an A/C to receive the broadcast channel (BCH) carrying the management information of the cell. At this point of operations the time advance correction is still missing. It is gained by transmitting a *net entry request* on the random access channel (RACH) and processing the GS's reply. If a positive acknowledgement has been received the A/C has reached SS 2 and may now use all services offered by the cell. In the context of the DLL the transition from SS1 to SS2 is referred to as *net entry.*

Protocol Stack

The B-VHF data link protocol is internally organized into several sub entities. Figure 4 shows a high level structure of the B-VHF protocol components.

The *medium access control* (MAC) sub-layer provides the higher protocol elements with access to the physical transport channels on the contention free slots FL and RL and manages the medium access algorithms of the other slots.

On the RL the MAC entity distinguishes between three different types of resource allocation: *permanent, reserved* and *on-demand*.

Permanent resource allocations are only used for the transmission of digital voice and are permanently associated to a physical transport channel with a specific GS and service (e.g. ATC-voice).

Resources for data applications have to be created when the need arises. Two types of reservations are allowed. *Reserved* allocations are intended for data applications with high demand and predictable transmission patterns; they grant an A/C a guaranteed bandwidth without medium access delay. All other data applications have to make reservations according to the amount of data to be transmitted. Those data link capacities are granted *on demand.*

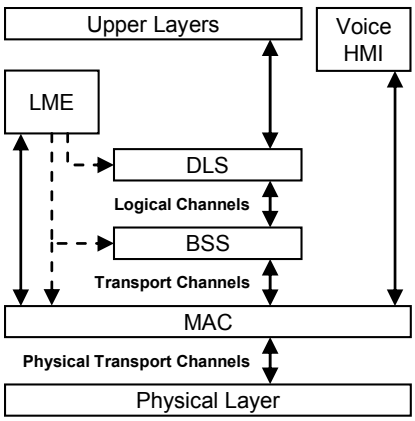

Figure 4. High level B-VHF DLL.

An A/C has to issue its reservation requests (limited to a maximum amount of data) in one of the sRA slots using a random delay counter algorithm. The sRA slots are further divided into several "user groups" to increase the throughput of the sRACH channel. The GS centrally coordinates all received resource requests for the RL according to their priority and issues grants on the FL. As the

FL and BC are used by the GS only, the resource management is handled by the GS.

The *B-VHF special service* (BSS) sub-layer manages channel access by scheduling frames for the appropriate slots and issuing resource requests to the LME. The BSS maintains the proper burst size by segmenting DLS packets into BSS frames suitable for the respective time slot.

The *data link service* (DLS) sub-layer is responsible for frame exchange, frame processing, error detection, error recovery, providing a suitable set of communication protocols to support offered services by the B-VHF system, and data encryption if desired. The link exchange protocol used for B-VHF is an HDLC derivate [9].

The *link management entity* (LME) controls link establishment and maintenance between peer DLS sub-layers. Additionally, the LME coordinates net-entry, net-exit, transparent cell handover, manual ATC sector handover, and failure handling procedures. The LME collects the resource requests of the BSS and sends the accumulated demand to the GS using the MAC.

Services and Interface to Upper Layers

The B-VHF data link has been designed to support voice and data applications simultaneously. Hence it provides the following services to the upper layers:

- Digital voice service – party line.
- Reliable and unreliable (e.g. streaming) connection oriented data transfer.
- Acknowledged and unacknowledged connectionless data transfer.

The B-VHF system has been designed to transparently support digital voice communication in entire ATC sectors.

If a sector is covered by a single cell the B-VHF data link directly supports this mode of voice communication. In the case that an ATC sector is covered by more than one B-VHF cell, the logically equivalent voice channels of all concerned cells can be interconnected to permanent virtual circuits over the ground network. By this means any number of B-VHF cells can be used to cover ATC sectors of arbitrary size while supporting transparent digital voice.

In order to emulate the party line functionality of the legacy DSB-AM system the exchange of voice messages is managed by the human supported *listen before push-to-talk* protocol.

It was a goal for the B-VHF system to support existing ATN applications and to be adaptable to new protocols. Consequently, the B-VHF interface to the upper layers has been designed according to current standards [10] supporting the ATN and IP internet protocol stacks and a raw data interface.

Simulation Setup

Each simulation setting consists of one B-VHF cell with up to 255 registered A/C. The A/C population (arrival and departure) and traffic patterns (voice and data) are derived from the three base scenarios *Parking, Take-Off & Landing*, and *En-route*.

Data traffic patterns are defined for all three air traffic scenarios and for the years 2015, 2020, and 2025. Extensive tables of the traffic patterns were presented in deliverable [11]. The required levels of quality of service can be found in the appropriate sections of the same deliverable.

The bit error rate (BER) simulated for the PHY layer was considered by means of frame error rate (FER) for the different transport channels FCH, RACH, and sRACH. The FER varies with the used modulation technique (which implies coding rate, frame length, spreading sequence, SNR, etc.). We investigated two modulations, namely QPSK and QAM64.

In the course of the definition of the simulation setting we decided to choose three significant levels of cell population. These populations have been carefully chosen to identify critical bottlenecks of the system and make an assessment of quality parameters possible.

For each of the three scenarios we defined one *low*, *medium*, and *high* population setting (exact parameters can be found in B-VHF deliverables [11] and [12]).

Each of these nine scenarios has been combined with the appropriate data traffic patterns

for the years 2015, 2020, 2025, and both modulations (QPSK, QAM64).

IV Simulation Results

PHY Layer

For the simulations the parameters described in Section II are used. According to the B-VHF specifications, the received B-VHF signal power P_s is ranging typically between -90 dBm and -50 dBm over all used subcarriers. The noise power is fixed to -110 dBm over 1 MHz.

In the net entry phase, the A/C must synchronize with the B-VHF signal with the S&C synchronizer. Therefore, the S&C algorithm uses the pilot synchronization symbol in the preamble of the FL frame. Because of the presence of interferers, the symmetry of the pilot symbol in the time domain may be affected, such that the S&C algorithm is not able to deliver a correct timing estimate. The occurrence of an incorrect estimate can be detected by evaluating the known pilot signal. After detection of an incorrect timing estimate, the S&C algorithm must wait for the pilot synchronization symbol in the next FL frame to obtain a new timing estimate. Hence, an incorrect estimate will cause a delay in starting up a new communication link. This delay will increase when the probability of an incorrect timing estimate increases; this probability turns out to be an increasing function of the total interference power. The time distance between two pilot synchronization symbols equals T_F=60 ms. Therefore, the average time to acquire initial timing is lower bounded by $T_F/2$=30 ms. In Table 5, the average delay in initial synchronization is shown for the different FL scenarios. It can be observed that in all cases, except FL-WC, synchronization will be successful in less than 1s. In the FL-WC case, the total interference power is very high, causing a large delay. However, this delay can be reduced if the number of pilot synchronization symbols per FL frame is increased, e.g. if the preamble contains four pilot symbols instead of one, the delay for the FL-WC case reduces to 800 ms.

Table 5. Average time to acquire initial timing in 99% of the cases, P_s=-87dBm.

	FL-PARK	FL-TOFF	FL-ENR	FL-WC
delay (ms)	300	50	200	1700

In the following, the performance of the B-VHF system is evaluated for the FL, in the cases of voice and data transmission in terms of BER and the transmission of information in the header in terms of frame error rate (FER). For voice transmission, the target BER equals 10^{-3}, while for data transmission the target BER=10^{-4}. The target FER for transmission in the header equals 10^{-3}.

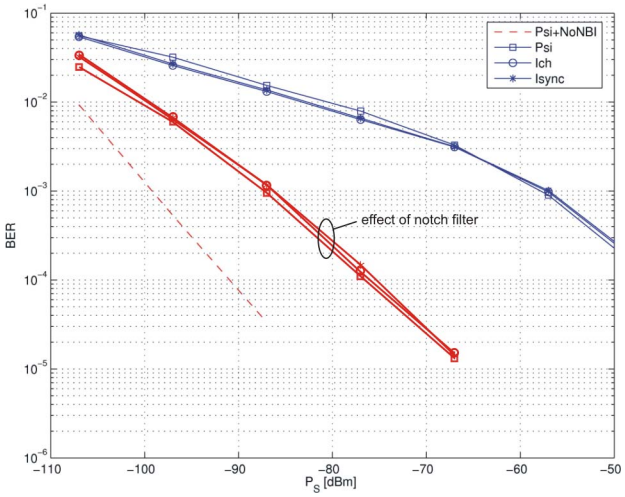

Figure 5. BER for FL-PARK, voice.

In Figure 5, the BER for voice transmission is shown for the FL-PARK scenario. When comparing the BER for the cases of ideal channel estimation and ideal synchronization (Psi), ideal synchronization and imperfect channel estimation (Ich), and imperfect channel estimation and synchronization (Isync), it can be observed that the proposed channel estimator and synchronizer work properly. In Figure 5, also the BER for the case where no interference is present is shown. From the result, it can be concluded that the interference causes a strong performance degradation, i.e. a loss of 43 dB at BER = 10^{-3}. To improve the performance, we have to remove (part of) the interference signal e.g. by notch filtering.

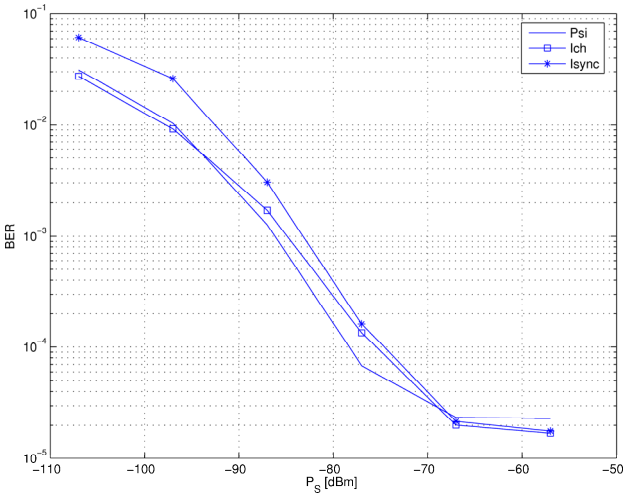

Figure 6. BER for FL-TOFF, voice.

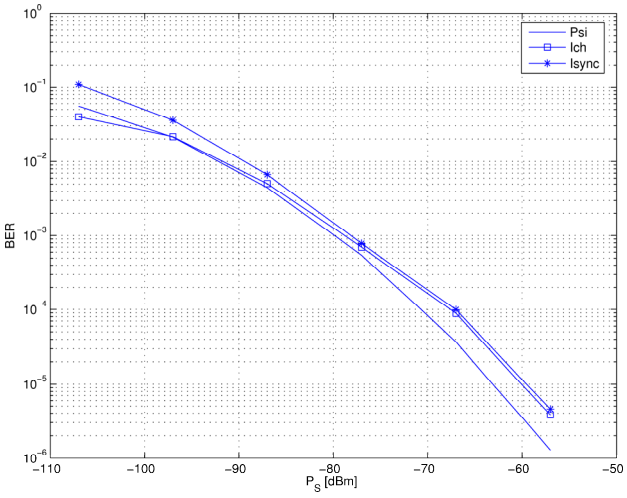

Figure 7. BER for FL-ENR, voice.

In Figure 6 to Figure 8, the BER for voice transmission for FL-TOFF, FL-ENR, and FL-WC is shown. It can be observed that the BER in these cases is better than for FL-PARK. This can be explained as the average power of the strong interferers in FL-PARK is 15-20 dB higher than in the other cases (see Table 3). Similarly, comparing FL-ENR and FL-WC, that are sharing the same channel model but have different interference model, it can be observed that the FL-WC case has worse performance because of the higher total interference power. Hence, canceling the interference by e.g. notch filtering will benefit the performance in all cases.

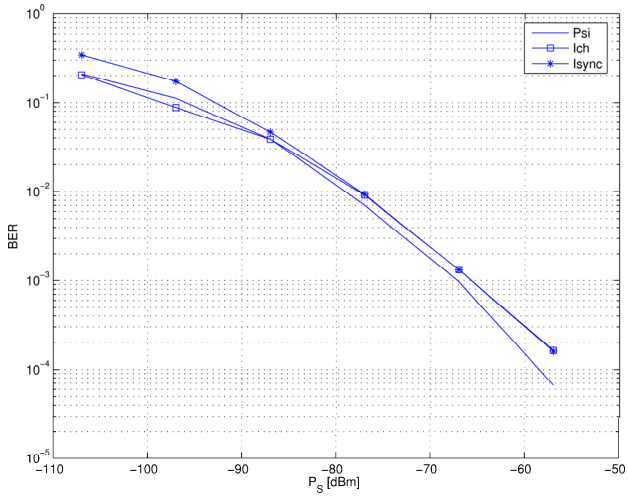

Figure 8. BER for FL-WC, voice.

InTable 6, the signal power P_s is shown for which the target BER/FER is achieved for voice and data transmission, and for transmission in the header in the FL. Similar conclusions can be drawn for data and header transmission as for voice transmission.

Table 6. Performance for the different FL simulation scenarios.

	FL-PARK	**FL-TOFF**	**FL-ENR**	**FL-WC**
voice (dBm)	-57	-75	-77	-65
data (dBm)	-51	-80	-80	-73
header (dBm)	-60	-91	-88	-80

As depicted in Table 6, the required received B-VHF signal power P_s is relatively high in all scenarios due to the high remaining interference. In order to reduce NBI different NBI mitigation techniques are applied for the FL-WC scenario, assuming perfect channel estimation and synchronization. As shown in Figure 9, in this scenario notch filtering of the six strong interferers does not lead to a significant improvement in system performance as the remaining influence of the seven weak interferers is still high. When strong and weak NBI is mitigated in frequency domain by means of leakage compensation with one observation subcarrier per interferer, P_s is improved to -84 dBm. When windowing is applied in addition, P_s is further reduced to -88 dBm. Compared to the case when only windowing is

applied, an improvement of 23 dB is achieved at the cost of additional computational effort and the loss of seven data subcarriers for NBI observation purposes.

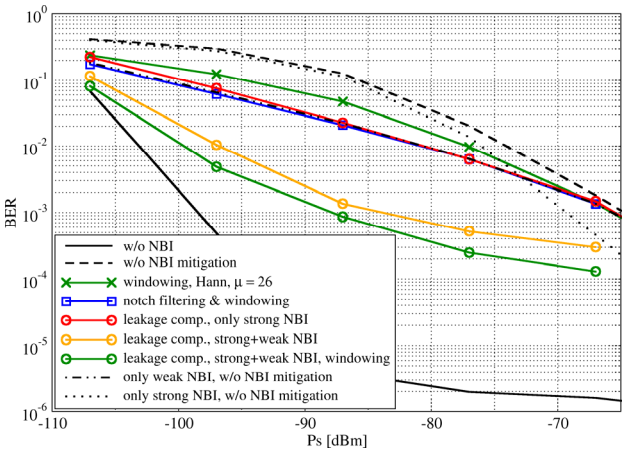

Figure 9. BER for FL-WC, voice, different NBI mitigation techniques.

MAC Simulation

This part of our performance evaluation discusses the medium access delay caused by the random access algorithms used for net initialization and resource acquisition. The results have been obtained by an event driven simulation implementing parts of the B-VHF protocol. In order to verify these simulations the same results have been derived with a Markov model of the used MAC algorithm. A formal discussion of this model can be found in [12].

Net Initialization

Our simulations show that the expected medium access delay for realistic scenarios is typically well below 1.0 seconds. This value is never exceeded until the A/C inter-arrival time surpasses 100 arriving A/C per minute, a value that will never be reached in reality.

Table 7. Net entry (SS1 to SS2).

Average Latency	95 % Latency	99 % Latency	99.996 % Latency
421 ms	588 ms	859 ms	1061 ms

This shows clearly that the second step of the net initialization (*synchronization on the RL*) can be conducted very quickly, satisfying all requirements.

Resource Requests

This part of our evaluation analyses the performance of resource acquisition on the RL. The achieved bandwidth utilization on the higher layers correlates strongly with the medium access delay suffered here.

Each sRA is internally decomposed into a number of slots in time and frequency. Access to these slots is managed by the well known *random delay counter* algorithm. It is known that the performance of this algorithm degrades significantly under excessive load (i.e. messages per slot). Therefore additional back-off mechanisms are required, although these timers need to be adjusted carefully to provide efficient means of recovery.

If the expected waiting time for successful medium access exceeds a certain threshold the bandwidth utilization drops significantly. The exact value of this threshold is dependent on the timer adjustment of the DLS protocols, as overdue resource requests and jitter produce timeouts in the DLS. To remedy this situation it is imperative to provide appropriate numbers of slots in each sRACH. Consequently, the aim of this section's simulation and theoretical analysis was to identify suitable configurations for all scenarios.

Figure 10 presents our results for an "En Route 2015" scenario with high, medium, and low cell population. The expected medium access delay increases almost exponentially when the amount of available slots decreases. Comparison of both parts of the figure shows that our analytical and simulation results correspond almost perfectly (over 0.94 correlation).

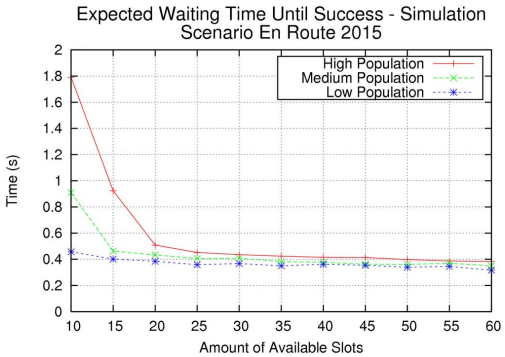

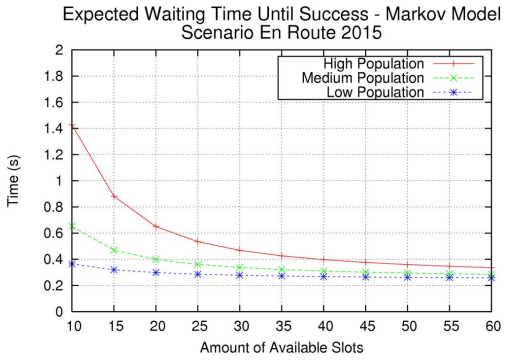

Figure 10. Simulation and theory output.

End-to-End Simulation

Voice System

The end-to-end performance of the voice system has been evaluated in a custom scenario as voice traffic is not influenced by data traffic. In order to simulate party line functionality this special scenario comprised a varying number of A/C communicating with each other (over relay) and the GS. Statistics have been collected for every completed one-way transmission, which implies that every relayed A/C transmission has been seen as two distinct voice messages. One message from A/C to ground and the other message from GS to all A/C.

The simulation results show that the B-VHF system supports digital voice with the required quality of service. All latencies are below 120ms.

Table 8. Voice latency statistics.

Average Latency	95 % Latency	99 % Latency	99.996 % Latency
63.74 ms	90.07 ms	113.13 ms	118.77 ms

Data Link

The end-to-end data traffic simulations have been performed with a constant number of users. As the maximum value for each scenario has been chosen, these results present worst case evaluations and thereby define upper bounds.

As an example service controller pilot data link communication (CPDLC) requires that 95% of the transmitted frames have a latency below 2 seconds and 99.996% have a latency below 5 seconds. The results presented in Table 9 show that these requirements can be fulfilled in most of the cases. The 99% latency is always below the required values. The exact results depend heavily on the chosen timeout values, which leaves much room for future optimizations. Complete results for all simulated scenarios and services can be found in [11].

Table 9. Simulation results for acknowledged CPDLC transmission; QAM64; 100 A/C; timers managed by Karn's algorithm [13].

	Year	Mean Latency (s)	95% Latency (s)	99% Latency (s)	99.996% Latency (s)
Airport	2015	0.401	1.549	2.178	4.199
	2020	0.413	1.536	3.229	4.435
	2025	0.660	2.091	4.009	8.215
En-Route	2015	0.405	1.655	2.279	4.174
	2020	0.441	1.776	2.522	4.404
	2025	0.594	1.912	3.336	6.135
Terminal	2015	0.422	1.525	2.322	4.644
	2020	0.477	1.730	3.043	7.268
	2025	0.634	1.817	4.022	6.854

V Assessment and Conclusions

In this paper, the overlay concept of the B-VHF system is assessed by means of simulations of the designed PHY and higher layers.

The simulations for the PHY layer in typical and worst-case interference scenarios have shown that a transmission of the B-VHF system even in presence of strong interference from legacy VHF systems is possible. The proposed synchronization algorithms work properly despite the high total interference power. However, the performance in terms of BER or FER can be improved with appropriate additional NBI mitigation techniques. That way the required transmission power and

consequently, the interference on legacy VHF systems, could be further reduced.

For the higher layer simulations realistic phases of flight from the PHY layer simulations as well as models of future air traffic have been considered. The designed MAC protocol enables a quick net entry and resource acquisition when a sufficient number of slots is available. The latency of voice and data links is determined in end-to-end simulations and meets the requirements of quality of service.

The simulations performed and discussed in this paper have validated the overall B-VHF overlay concept. With further refinements and optimizations the B-VHF system is a promising candidate for aeronautical communications meeting the requirements of future air traffic control systems.

References

[1] http://www.b-vhf.org

[2] M. Schnell, E. Haas, C. Rihacek, and M. Sajatovic, "B-VHF – An Overlay System Concept for Future ATC Communications in the VHF Band," *Proc. 23rd Digital Avionics Systems Conf. (DASC 2004)*, Salt Lake City, USA, Oct. 2004.

[3] I. Cosovic, S. Brandes, M. Schnell, and B. Haindl, "Physical Layer Design for a Broadband Overlay System in the VHF Band," *Proc. 24th Digital Avionics Systems Conf. (DASC 2005)*, Washington D.C., USA, Oct. 2005.

[4] A. Redfern, "Receiver Window Design for Multicarrier Communication Systems," *IEEE Journal on Selected Areas in Communications*, Vol. 20, No. 5, 2002, pp.1029-1036.

[5] J. Schwarz and S. Brandes, "Leakage Compensation in an OFDM Overlay System for DSB-AM Aircraft Radio," *Proc. of 10th International OFDM Workshop*, Hamburg, Germany, Aug. 2005, pp. 240-244.

[6] H. Steendam and M. Moeneclaey, "Sensitivity of orthogonal frequency-division multiplexed systems to carrier and clock synchronization errors," *Signal processing*, Vol. 80, No 7, July 2000, pp. 1217-1229.

[7] M. Guenach, H. Wymeersch, H. Steendam, and M. Moeneclaey, "Code-aided ML joint synchronization and channel estimation for downlink MC-CDMA", *IEEE Journal on Selected Areas in Communications, special issue on MC-CDMA*, Vol. 24, No 6, June 2006, pp. 1105-1114.

[8] T.M. Schmidl and D.C. Cox, "Robust frequency and timing synchronization for OFDM," *IEEE Transactions on Communications*, Vol. 45, No 12, Dec. 1997, pp. 1613-1621.

[9] "Information technology – Telecommunications and information exchange between systems – High-level data link control (HDLC) procedures," ISO/IEC 13239, 3rd Edition, July 2002.

[10] "Information technology – Open Systems Interconnection – Network service definition," International Standard 8348, Apr. 1987.

[11] "Performance Evaluation of the Upper Layers" of the B-VHF project, report D25, project number AST3-CT-2003-502910.

[12] "Performance Evaluation of the B-VHF DLL" of the B-VHF project, report D24, project number AST3-CT-2003-502910.

[13] P. Karn, and C. Partridge, "Improving Round Trip Time Estimates in Reliable Transport Protocols," *Proceedings of ACM SIGCOM'87,* August 1987.

Email Addresses

Sinja.Brandes@dlr.de

Michael.Schnell@dlr.de

roki@cosy.sbg.ac.at

mehammer@cosy.sbg.ac.at

tgraeupl@cosy.sbg.ac.at

Heidi.Steendam@UGent.be

Mamoun.Guenach@telin.ugent.be

Christoph.Rihacek@frequentis.com

Bernhard.Haindl@frequentis.com